

Lecture 5: Interfacial Crystallography I

The structure of surfaces and surface free energy

Every real crystal must have at least one imperfection – its surface. It is useful to introduce crystal interfaces by thinking of a surface that is parallel to a prominent crystallographic plane and represents a smooth sheet of atoms of which the pattern is the same as that of a parallel plane inside the crystal. We shall use this simple clear idea, but recognise it is not strictly true.

Surfaces show the phenomenon of *reconstruction*, whereby even in high vacuum the outer layers of atoms rearrange into a more energetically favourable situation. A well-known example is the 7×7 structure found on (111) Si. Similar surface reconstructions occur on clean metal surfaces. These reconstructions can be rationalised in terms of the coordination of the atoms at the surface and the electronic structure at the surface being different from the bulk (which, in practice, typically means distances of > 1 nm from the surface).

Rather than such outer surfaces, we are concerned here with *internal* interfaces in crystalline solids, e.g., grain boundaries and boundaries between different phases, such as epitaxial interfaces.

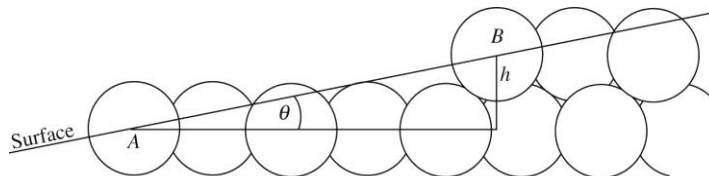
Surface energy

Atoms at a surface are deprived of some of their neighbours. Since the binding of an atom to its neighbours contributes a favourable negative term to the energy of a crystal, we can attribute some excess energy to the presence of the surface.

Imagine two identical surfaces to have been created within a single crystal by breaking the atomic bonds through which a plane passes. The surface energy is then equal to half the energy of the broken bonds. (This equation assumes that the energies of those bonds which are left do not change.) The idea of broken bonds is useful in discussing how the energy of a surface will change as it is rotated out of a low-index orientation.

Suppose a {111} surface of a c.c.p. metal is rotated through a small angle θ about a $\langle 1\bar{1}0 \rangle$ direction. It is apparent from the figure below that it then contains a density of steps ρ per unit length:

$$\rho = \frac{\sin \theta}{h}$$



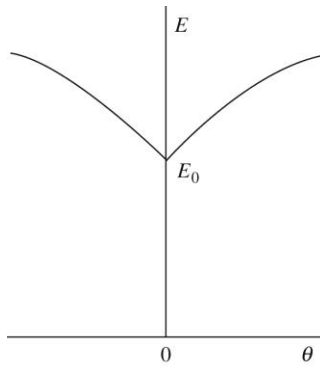
Surface at a small angle θ to a {111} plane of a c.c.p. metal.
The surface is normal to the plane of the figure.

where h is the spacing of the {111} lattice planes.

If the angle θ happens to be such that the points A and B in the figure on the previous page lie on $\langle 1\bar{1}0 \rangle$ rows of atoms, then the steps will be evenly spaced. For other surfaces of rational orientation, the steps can occur in evenly-spaced groups, but if the surface is irrational, there must be irregularities in the arrangement of steps. An atom on a step lacks more neighbours, and so has more broken bonds, than an atom in the flat $\{111\}$ surface; consequently the steps introduce an extra energy which is proportional to the number of steps, as long as they are so far apart that they do not interact with one another. If each step contributes an energy β per unit length, then the total energy of unit area of surface is

$$E = E_0 \cos \theta + \frac{\beta \sin |\theta|}{h}$$

where E_0 is the energy of unit area of $\{111\}$ surface. The surface energy therefore increases as the surface is rotated from its low-index orientation, in either sense. The plot of energy as a function of θ shows a cusp at which $dE/d\theta$ changes discontinuously from $-\beta/h$ to $+\beta/h$:



A schematic of energy E as a function of angle θ away from a low-index plane

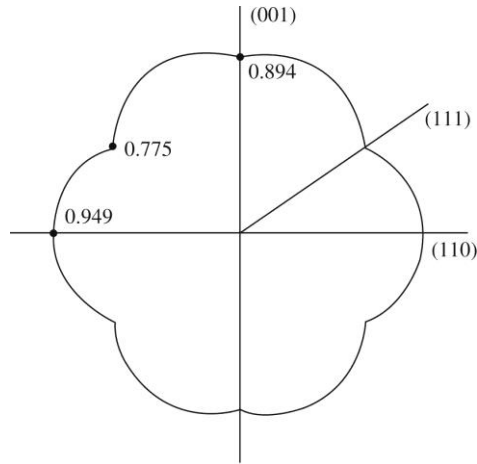
Similar arguments can be applied to a small rotation of the $\{111\}$ surface about any axis; therefore a cusp exists in a three-dimensional plot of surface energy against orientation. Such a plot may take the form of a polar diagram in which the energy of a surface is represented by a vector which is normal to the surface and of length in proportion to the energy of the surface. The energy plot can be expected to exhibit a number of cusps at the orientations of various low-index planes.

The energy of a surface is closely related to its surface free energy, defined as the work that can be obtained from the destruction of unit area of surface. The surface free energy is

$$\gamma = E - TS$$

and although the energy E is usually its more important component, the entropy term TS can be significant. For example, the steps upon a surface that is slightly off a low-index plane will introduce a configurational entropy, because their straightness and spacing may vary. Therefore, at a finite temperature, the cusp in the surface free energy plot will not be as sharp as that in the energy plot and it may even disappear for higher-index planes.

A polar diagram of surface free energy is called a γ -plot. A $(1\bar{1}0)$ section through the γ -plot of a c.c.p. metal is shown below, as computed from a simple nearest neighbour bond model.



Possible $(1\bar{1}0)$ section through the γ -plot of a c.c.p. metal. Values given are in units of the surface energy of a $\{210\}$ surface (from J. K. Mackenzie *et al.* (1962)).

Structure and energy of grain boundaries

A crystalline solid is usually found in the form of a polycrystal, i.e. an aggregate of randomly oriented single crystals, called grains. Even so-called single crystals usually contain regions called subgrains, which have slightly different orientations.

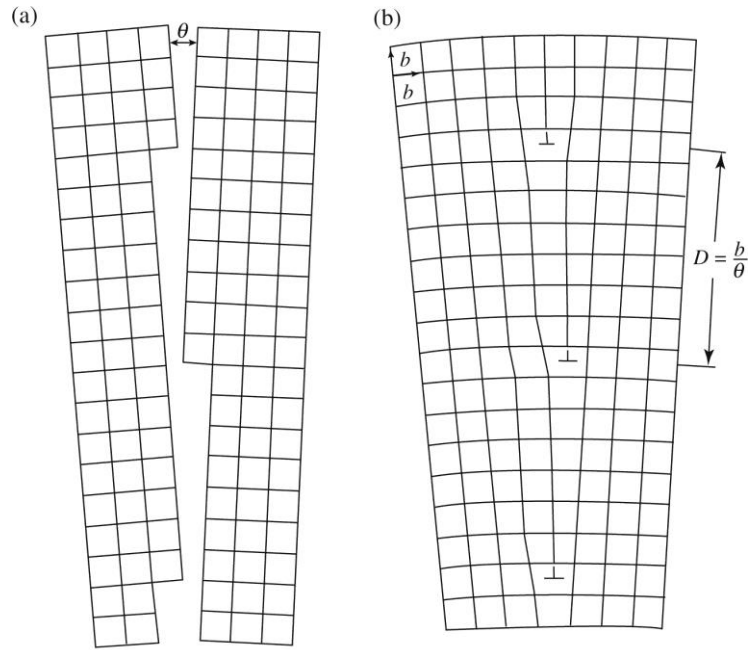
Low angle tilt grain boundaries

Probably the simplest type of grain boundary to visualize is the symmetrical low angle *tilt boundary*, where the two grains on either side are related by symmetrical rotations about an axis lying in the boundary, and where the rotation is relatively small ($< 10^\circ$). A low angle tilt boundary in a simple cubic structure is shown overleaf. This boundary could be formed by joining two crystals having unrelaxed stepped surfaces which are rotated from a cube plane by small angles $+\theta/2$ and $-\theta/2$ about a $\langle 100 \rangle$ direction (a). When the two surfaces are joined, these steps in them become edge dislocations, with the Burgers vector equal to the step height, as in the schematic in (b). For small θ

$$d \approx \frac{b}{\theta}$$

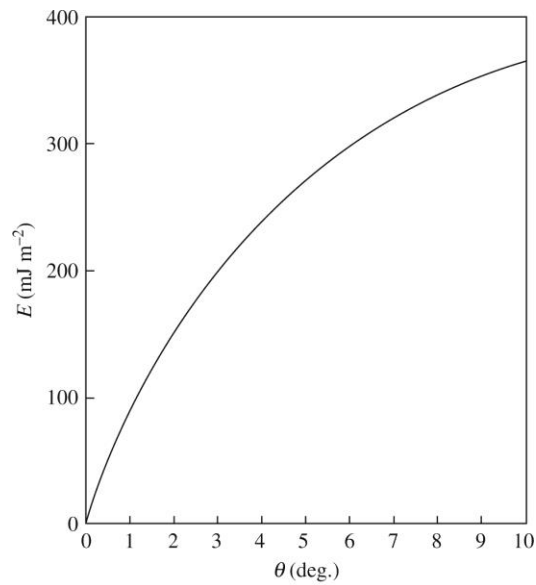
Read and Shockley have calculated the energy of such an array in an infinite isotropic medium. They found the energy per unit area to be of the form

$$E = E_0\theta(A_0 - \ln \theta)$$



Low angle symmetrical tilt boundary in a simple cubic lattice.
The boundary is normal to the plane of the figure.

This equation can be applied only to boundaries having a small angle of tilt, θ typically less than 10° such that the cores of the dislocations do not overlap. The energy of a tilt boundary rises steeply as its angle increases from zero because the strain field of each dislocation spreads out to a very large distance when the dislocations are widely separated. The increase in energy becomes less steep as the angle of tilt increases further because the stress fields of the dislocations cancel as they come closer together.



Example of the energy of a tilt boundary as a function of the tilt angle θ .

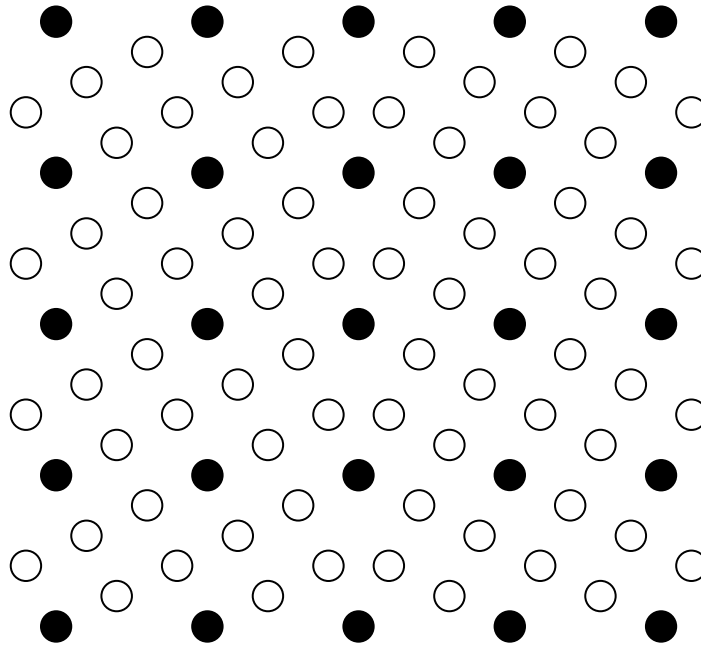
High angle tilt grain boundaries

Shallower cusps in the grain boundary energy must exist at angles of tilt at which the dislocations are evenly spaced, as suggested in the early work on computer modelling of grain boundaries by Hasson *et al.* in the 1970s. This is also consistent with the trends seen in later, more detailed, atomistic studies of the structure of symmetrical tilt grain boundaries in c.c.p. metals.

For example, when $\cot \theta/2 = 2$ (or $\theta \approx 53.1^\circ$), a hard sphere model (i.e., a purely geometrical model) of the structure of the boundary is neat and regular, as shown in the figure below. The plane of the boundary is a $\{210\}$ plane in either grain, and one grain can be described as a twin of the other, with the twin plane $K_1 = (210)$.

Since the atoms in the twin boundary lie on the lattices of both grains in this purely geometrical model, we may expect the energy to be particularly small when the density of atoms on this boundary is high, i.e. when K_1 is a low-index plane. Since (210) is the closest packed twin plane that can be formed in the simple cubic lattice when the tilt axis is [001], the deepest of the energy cusps should occur here, at the angle $\theta \approx 53.1^\circ$.

Atomistic calculations confirm this qualitative picture: in copper and aluminium, the boundary modelled in the figure below is a favoured boundary, in that (i) the units of structure which exist in this boundary are small, and (ii) symmetrical tilt grain boundaries at other angles of rotation about [001] have mixtures of this unit of structure and that of another favoured orientation at $\theta = 90^\circ$.



Schematic of a high angle tilt boundary of good fit between one grain on the left and one grain on the right in a simple cubic material. The boundary plane is vertical and normal to the plane of the figure. The dark circles represent atoms that lie on points of the lattices of both grains.

This is an example of a *coincidence lattice orientation*. Other examples are shown in the table on the next page.

Table 13.2 Some coincidence lattices for c.c.p. and b.c.c. crystals [21]

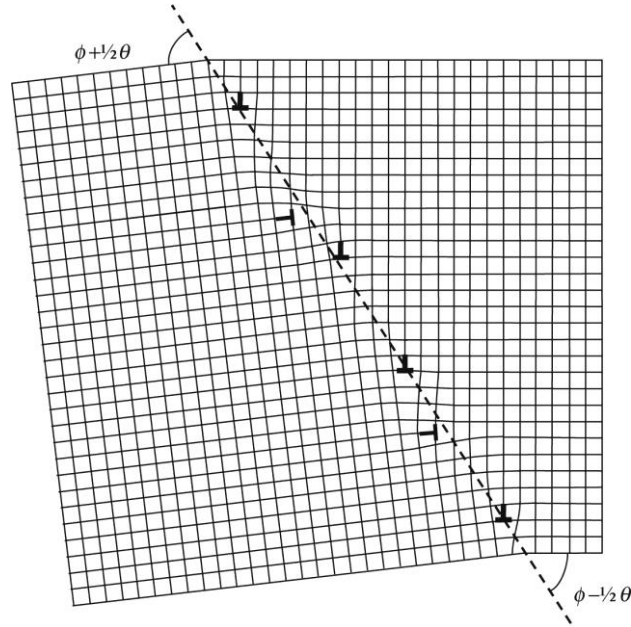
Fraction of lattice points on coincidence lattice	Rotations producing coincidence lattice		Closest-packed plane of coincidence lattice written as plane of parent lattice	
	Axis	Angle (°)	c.c.p.	b.c.c.
1 : 3	110	70.5	111	112
	111	60		
	210	131.8		
	211	180		
	311	146.4		
1 : 5	100	36.9	210	310
	210	180		
	211	101.6		
	221	143.1		
	310	180		
	311	154.2		
	331	95.7		
1 : 7	111	38.2	123	123
	210	73.4		
	211	135.6		
	310	115.4		
	320	149		
	321	180		
	331	110.9		

Low angle asymmetrical tilt grain boundaries

A low angle tilt boundary can be turned out of its symmetrical orientation by rotating it about the tilt axis, so that it becomes a low angle asymmetrical tilt grain boundary. The effect of a rotation of χ is shown in the diagram on the next page. Edge dislocations with extra planes that are normal to those of the original set are introduced. The energy of the boundary has the same form as for the low angle symmetrical tilt grain boundary,

$$E = E'_0\theta(A - \ln \theta)$$

where E'_0 is a function of ϕ . A sharp energy cusp occurs at the symmetrical orientation when $\phi = 90^\circ$.



An asymmetrical tilt boundary in a simple cubic lattice where the misorientation across the boundary is θ . The boundary makes an angle of $90^\circ - \phi$ with the symmetrical tilt orientation

High angle asymmetrical tilt grain boundaries

A qualitatively similar cusp should exist for a high-angle tilt boundary which is a twin plane, since rotating such a boundary out of its symmetrical position destroys the good fit of the atoms upon it.

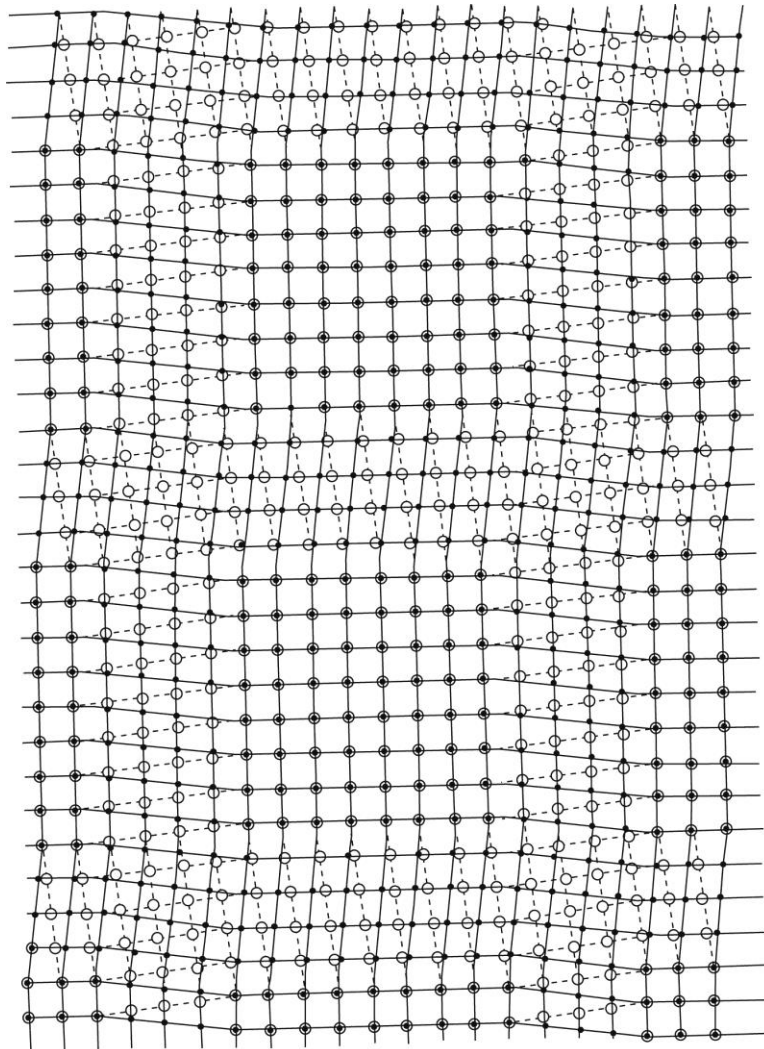
Atomistic simulations of asymmetrical high-angle tilt grain boundaries confirm this to be so: cusps occur in the energy against misorientation at both favoured boundary and ‘multiple unit reference structure’ orientations.

A high-angle tilt boundary which is a twin plane is an example of both a favoured boundary and one which has a favoured multiple unit reference structure.

Low angle twist grain boundaries

A low-angle twist grain boundary consists of a grid of screw dislocations, as shown in the diagram below. The deformation due to one of the two orthogonal sets of screw dislocations is such that its pure shear component cancels that of the other set at large distances from the boundary, whereas its rotational component adds to that of the other set and produces the necessary relative rotation of the grains.

The energy of a twist boundary will increase with the angle of twist in the same general way as the energy of a tilt boundary increases with the angle of tilt.



A low angle twist boundary in a simple cubic lattice.
The boundary is parallel to the plane of the figure.

High angle twist grain boundaries

The energy of a twist boundary will increase with the angle of twist in the same general way as the energy of a tilt boundary increases with the angle of tilt. The energy should be cusped at those angles of twist at which the atoms fit together well at the boundary. Again, to begin an understanding of such boundary, the concept of the *coincidence site lattice* (CSL) is useful, but to determine relative energies of twist grain boundaries, we need atomistic simulations.

The coincidence lattice therefore provides a useful way of *grouping together* various boundaries of good fit between grains having the various equivalent orientation relationships that produce the same coincidence lattice in high symmetry materials.

Detailed atomistic calculations on the structure of high-angle twist boundaries in c.c.p. metals confirm that the simple geometrical picture is useful, even if the actual relaxed structure computed for such boundaries is more complicated, involving small volume increases at the boundaries, relaxations parallel to the boundaries, and also translations parallel to the boundaries.

General grain boundaries

Orientation relationships between any two different grains (and lattices in general) can be described geometrically in terms of either coincident cells or *near-coincident* cells; the presumption being that such orientations are more likely to be favoured than other orientations.

However, Sutton and Balluffi conclude that there is a lack of quantitative evidence that a geometric criterion of ‘good fit’ between lattices, however described, is actually useful for making predictions about low energy interfaces. Instead, they state that details of the interfacial structure and the nature of the atomic bonding in a particular situation have to be taken into consideration when attempting to predict low interfacial energies.

The alternative viewpoint is that, notwithstanding the conclusions of Sutton and Balluffi, energy minimisation does correlate with geometrical features, such as good atom matching across interfaces.

This viewpoint is inspired by work such as that of Shiflet and van der Merwe on interfaces between c.c.p. and b.c.c. crystals in which (111) interfaces of c.c.p. crystals are forced to be parallel to (110) b.c.c. interfaces.

In such circumstances, geometrical features such as row matching are found to correspond to energy minimisation, albeit not through an atomistic simulation analysis, but through instead an analysis of the energy savings to be made from the introduction of structural ledges as misfit-compensating defects.

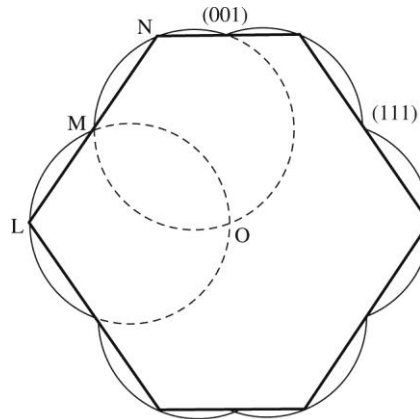
The shapes of crystals and grains

Although the shape of a crystal is usually a consequence of the way in which it grew, or perhaps of its cleavage, there must nevertheless be some equilibrium shape that might be reached in practice by an unconstrained small crystal or by a small void within a crystal. This shape is determined by the surface free energy γ and is such as to minimize the total free energy, i.e.

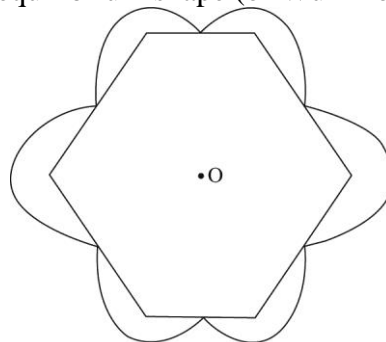
$$\int_A \gamma \, dA = \text{a minimum}$$

If the surface free energy is isotropic, then the equilibrium shape is a sphere; i.e. the surface area of a given volume is minimized. If the surface free energy varies with orientation, then the equilibrium shape can be derived from the γ -plot by means of a theorem due to Wulff.

The equilibrium shape, often referred to as a Wulff plot, is that of the inner envelope of planes normal to, and passing through the ends of, the vectors representing surface free energies on the γ -plot ('Wulff planes'). The proof of Wulff's theorem for a body of fixed volume is non-trivial.

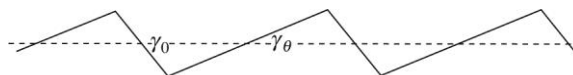


Example of the equilibrium shape (or Wulff form) of the crystal

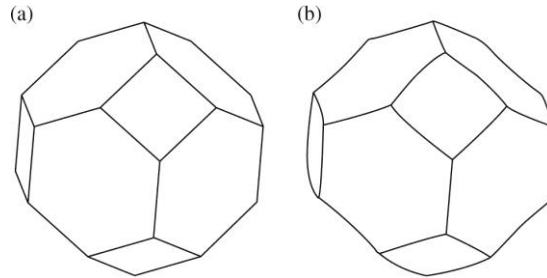


The same equilibrium shape as shown above, arising from a different γ -plot

An ordinary-sized crystal of arbitrary shape never reaches its equilibrium shape in practice, because of the large redistribution of material required and the small amount of energy to be gained thereby. Instead, a surface of an orientation not represented on the Wulff form can always reduce its total surface free energy by faceting, where the facets have low energy, e.g. schematically:



The arrangement of the grains within a polycrystal is observed to be quite similar to that of bubbles within a froth. This suggests that the pattern of grains is governed by grain boundary tensions, just as the pattern of bubbles in a froth is governed by the surface tension of the liquid between the bubbles.



(a) Truncated octahedron and (b) distorted truncated octahedron which, when stacked, meets the requirement that the surface tensions balance at all junctions.

Boundaries between different phases

Like a grain boundary, the boundary between two different crystalline phases can be specified by describing the orientation relationship between the lattices of the two crystals and the orientation of the boundary itself.

Corresponding to grain boundaries of special orientation, such as twin boundaries, there are special boundaries between two different crystals in a specific orientation relationship; corresponding to high angle grain boundaries, there are interfaces between randomly oriented crystals of different kinds.

Examples of special orientation relationships between two phases are the Kurdjumow-Sachs and Nishiyama-Wassermann orientation relationships found between austenite and martensite in steels and discussed in the next lecture. These orientation relationships, and variants of these orientation relationships, are also found in diffusional phase transformations between c.c.p. and b.c.c. phases.

The concepts relevant to an understanding of grain boundaries are also relevant to boundaries between different phases, e.g. the concepts of fit and misfit. Unfortunately, atomistic simulations of interphase boundaries are in their infancy because of the need to have reliable atomic potentials when modelling the boundaries, and so geometric criteria, however questionable, are often still the only criteria to hand when attempting to understand experimental observations of observed orientation relationships and ‘preferred’ interface planes.

Bollmann's 0-lattice theory

An important geometrical model relevant to interfacial crystallography is the 0-lattice¹ theory developed by Walter Bollmann (1920–2009). In this theory, lattices either side of a boundary are designated 1 and 2. It is then envisaged that these two crystal lattices are related point by point so that a vector designated $\mathbf{x}^{(1)}$ when expressed in the basis of lattice 1 is related to a vector $\mathbf{x}^{(2)}$ when expressed in the basis of lattice 2 through an equation of the form

$$\mathbf{x}^{(2)} = \mathbf{A}\mathbf{x}^{(1)}$$

where \mathbf{A} can be any form of homogeneous linear transformation such as a rotation, a shear or an expansion, or a combination of one or more of these. For grain boundaries, it is evident that \mathbf{A} is a rotation.

The 0-lattice formalism then generates an equation for the closure failure \mathbf{b} of an initial closed Burgers circuit around a vector \mathbf{p} lying in an interface between two lattices. In lattice 1, this closure failure is determined by the equation

$$\mathbf{b} = (\mathbf{I} - \mathbf{A}^{-1}) \mathbf{p}$$

where it is understood that \mathbf{b} and \mathbf{p} are defined in lattice 1. When the set of vectors \mathbf{b} are translation vectors of lattice 1, they form a lattice, designated by Bollmann the b -lattice. Bollmann designates such vectors $\mathbf{b}^{(L)}$, where the superscript L signifies lattice. The corresponding vectors \mathbf{p} which give rise to such vectors $\mathbf{b}^{(L)}$ are termed 0-lattice vectors – such vectors connect an 0-point at the origin to other 0-points on the 0-lattice. These 0-lattice vectors are written $\mathbf{x}^{(0)}$. With these definitions, we arrive at the equation

$$\mathbf{b}^{(L)} = (\mathbf{I} - \mathbf{A}^{-1}) \mathbf{x}^{(0)}$$

This is the basic 0-lattice equation. With this equation it is possible to model the dislocation structure of low-angle grain boundaries, coincidence site lattice orientations and interphase boundary structures.

This equation is a special quantised form of the more general form of the equation familiar in the formal theory of surface dislocations developed by Bilby and Bullough:

$$\mathbf{b} = (\mathbf{S}_1^{-1} - \mathbf{S}_2^{-1}) \mathbf{p}$$

where \mathbf{p} is a vector in the interface, \mathbf{S}_1 and \mathbf{S}_2 are the homogeneous linear transformations carrying the reference lattice in which \mathbf{b} and \mathbf{p} are expressed, into the final orientations of the '1' and '2' lattices respectively.

¹ pronounced 'oh lattice' rather than zero lattice.

Application of 0-lattice theory to low-angle grain boundaries

For low-angle grain boundaries \mathbf{A} is a rotation matrix. If we examine the simple case where the rotation is a rotation about [001] for a simple cubic lattice, as in the figure on page 79, then with respect to the left-hand grain,

$$\mathbf{A} = \begin{bmatrix} \cos \theta & \sin \theta & 0 \\ -\sin \theta & \cos \theta & 0 \\ 0 & 0 & 1 \end{bmatrix}$$

for a *clockwise* rotation of θ about [001] to rotate the left-hand grain into the right-hand grain (see the Appendix, page 91), so that

$$\mathbf{A}^{-1} = \begin{bmatrix} \cos \theta & -\sin \theta & 0 \\ \sin \theta & \cos \theta & 0 \\ 0 & 0 & 1 \end{bmatrix}$$

and

$$\mathbf{I} - \mathbf{A}^{-1} = \begin{bmatrix} 1 - \cos \theta & \sin \theta & 0 \\ -\sin \theta & 1 - \cos \theta & 0 \\ 0 & 0 & 0 \end{bmatrix}$$

If the angle θ is small, as it will be for low-angle grain boundaries, we can make the approximations $\cos \theta \approx 1$ and $\sin \theta \approx \theta$ to first order in θ , with θ in radians. Therefore, under these circumstances

$$\mathbf{b}^{(L)} = \begin{bmatrix} 0 & \theta & 0 \\ -\theta & 0 & 0 \\ 0 & 0 & 0 \end{bmatrix} \mathbf{x}^{(0)}$$

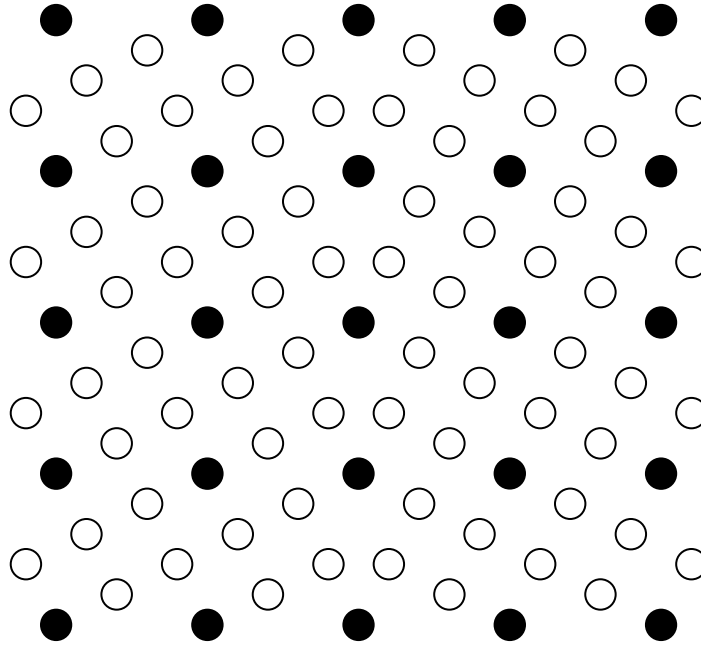
Hence, if $\mathbf{x}^{(0)}$ is the vector [001], $\mathbf{b}^{(L)}$ is zero, i.e., there is perfect registry of the two lattices along [001], as we would expect because this is the axis around which lattice (2) is rotated with respect to lattice (1). If $\mathbf{b}^{(L)}$ is $[\bar{b}00]$, $\mathbf{x}^{(0)}$ is the vector $[0, b/\theta, 0]$, i.e., the length of this 0-lattice vector defines the distance between edge dislocations in a low-angle tilt grain boundary.

Similarly, low-angle twist grain boundaries where the interface plane is (001) will consist of a square dislocation network. For example, along the direction $[0, b/\theta, 0]$ the total Burgers vector content will be $[b00]$ arising from a dislocation whose line direction is parallel to its Burgers vectors, i.e., arising from a screw dislocation. Likewise, along the direction $[-b/\theta, 0, 0]$ the total Burgers vector content will be $[0b0]$, also arising from a single screw dislocation.

For an asymmetrical tilt grain boundary, the Burgers vector content of the interface described by the equation $\mathbf{b}^{(L)} = (\mathbf{I} - \mathbf{A}^{-1}) \mathbf{x}^{(0)}$ can be quantised into sets of dislocations with Burgers vectors $[b00]$ and sets of dislocations with Burgers vectors $[0b0]$, as shown schematically in the diagram on page 82.

Application of 0-lattice theory to a coincidence site lattice orientation

To conclude this first lecture on interfacial crystallography, it is instructive to consider how 0-lattice theory can be applied to the coincidence site lattice orientation sketched on page 80 of these lecture notes, reproduced below:



Schematic of a high angle tilt boundary of good fit between one grain on the left and one grain on the right in a simple cubic material. The boundary is normal to the plane of the figure. The dark circles represent atoms that lie on points of the lattices of both grains. Here, Σ , the ratio of the volumes of the primitive coincidence cell and the primitive crystal lattice unit cell, is 5.

Here, the right-hand grain is rotated about a clockwise angle $\theta \approx 53.1^\circ$ about an axis normal to the page with respect to the left-hand grain – an angle where $\cot \theta/2 = 2$, $\cos \theta = 0.6$ and $\sin \theta = 0.8$. If we take the rotation axis to be $[001]$ with respect to the left-hand grain,

$$\mathbf{b}^{(L)} = \begin{bmatrix} 1 - \cos \theta & \sin \theta & 0 \\ -\sin \theta & 1 - \cos \theta & 0 \\ 0 & 0 & 0 \end{bmatrix} \mathbf{x}^{(0)}$$

(see the Appendix on page 91). Therefore, just as for the low-angle grain boundaries discussed on page 88, for this coincidence site lattice, the 0-lattice is a lattice of lines all parallel to $[001]$ intersecting the (001) plane perpendicular to $[001]$ in various positions on a two-dimensional grid of points defined with respect to the basis vectors $[100]$ and $[010]$ of lattice 1 perpendicular to $[001]$. We can define these positions by examining the equation

$$\mathbf{b}^{(L)} = \begin{bmatrix} 1 - \cos \theta & \sin \theta \\ -\sin \theta & 1 - \cos \theta \end{bmatrix} \mathbf{x}^{(0)}$$

where it is understood that $\mathbf{b}^{(L)}$ and $\mathbf{x}^{(0)}$ here are vectors in two dimensions. The determinant of the 2×2 matrix here is $2(1 - \cos \theta)$. Inverting the equation, we therefore have:

$$\mathbf{x}^{(0)} = \begin{bmatrix} \frac{1}{2} & -\frac{1}{2} \cot \theta/2 \\ \frac{1}{2} \cot \theta/2 & \frac{1}{2} \end{bmatrix} \mathbf{b}^{(L)}$$

using standard half-angle formulae. When $\cot \theta/2 = 2$, this becomes

$$\mathbf{x}^{(0)} = \begin{bmatrix} \frac{1}{2} & -1 \\ 1 & \frac{1}{2} \end{bmatrix} \mathbf{b}^{(L)}$$

If we represent the most general form of disregistry $\mathbf{b}^{(L)}$ as the vector $[n, m]$ where n and m are integers, then the two-dimensional grid defining where the lattice of 0-lines intersects (001) is the grid of vectors $[\frac{1}{2}n - m, n + \frac{1}{2}m]$.

If n and m are both even, this vector will be a crystal lattice vector, e.g., if $n = 2$ and $m = -4$, $\mathbf{x}^{(0)} = [5, 0]$; if $n = 4$ and $m = 2$, $\mathbf{x}^{(0)} = [0, 5]$; if $n = 0$ and $m = -2$, $\mathbf{x}^{(0)} = [2, -1]$, and if $n = 2$ and $m = 0$, $\mathbf{x}^{(0)} = [1, 2]$.

It is evident that the two-dimensional grid of points defined when n and m are both even is the set of coincidence lattice points in the diagram on page 89. This illustrates a general result: all coincidence lattice points are 0-lattice points, irrespective of the value of Σ , the ratio of the volumes of the primitive coincidence cell and the primitive crystal lattice unit cell, but not visa-versa.

Thus, for example, if we consider a $\Sigma = 37$ coincidence site lattice where the rotation angle θ is $\arccos(35/37) \approx 18.92^\circ$ about $[001]$, $\cot \theta/2 = 6$ so that

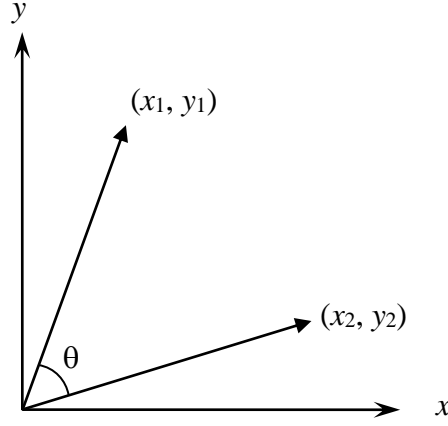
$$\mathbf{x}^{(0)} = \begin{bmatrix} \frac{1}{2} & 3 \\ -3 & \frac{1}{2} \end{bmatrix} \mathbf{b}^{(L)}$$

so that when $n = 2$ and $m = 12$, $\mathbf{x}^{(0)} = [37, 0]$; if $n = -12$ and $m = 2$, $\mathbf{x}^{(0)} = [0, 37]$.

These simple geometrical considerations imply that coincidence site lattices are ‘special’, but it is evident that some coincidence site lattice orientations might well be expected to be more special than others. We shall consider this further in the final lecture.

Appendix: Rotation matrix for a clockwise rotation of θ about [001] in a cubic material

For such a rotation it is evident that components of vectors along [001] remain unchanged. Therefore, we need only examine the effect of this rotation in the plane perpendicular to [001], i.e., in (001):



If we consider the rotation of a point initially defined as (x_1, y_1) to a new position (x_2, y_2) considered with respect to fixed x - and y -axes, we can define x_1 and y_1 in terms of a length r and an angle ϕ :

$$\begin{aligned} x_1 &= r \cos \phi \\ y_1 &= r \sin \phi \end{aligned}$$

so that

$$\begin{aligned} x_2 &= r \cos (\phi - \theta) = r \cos \phi \cos \theta + r \sin \phi \sin \theta = x_1 \cos \theta + y_1 \sin \theta \\ y_2 &= r \sin (\phi - \theta) = r \sin \phi \cos \theta - r \cos \phi \sin \theta = -x_1 \sin \theta + y_1 \cos \theta \end{aligned}$$

or, in matrix algebra formulation,

$$\begin{bmatrix} x_2 \\ y_2 \end{bmatrix} = \begin{bmatrix} \cos \theta & \sin \theta \\ -\sin \theta & \cos \theta \end{bmatrix} \begin{bmatrix} x_1 \\ y_1 \end{bmatrix}$$

i.e.,

$$\begin{bmatrix} x_2 \\ y_2 \end{bmatrix} = \mathbf{R} \begin{bmatrix} x_1 \\ y_1 \end{bmatrix}$$

for a two-dimensional matrix \mathbf{R} which has the property that its transpose, $\tilde{\mathbf{R}}$, is equal to its inverse, \mathbf{R}^{-1} , and the further property that its determinant is unity. For the three-dimensional form of the matrix, it is evident that it is given by the expression

$$\mathbf{R} = \begin{bmatrix} \cos \theta & \sin \theta & 0 \\ -\sin \theta & \cos \theta & 0 \\ 0 & 0 & 1 \end{bmatrix}$$

for a clockwise rotation about [001], as quoted on page 88.